

Electronic Structure Modulation via Curvature Engineering Enables C–C/C–N Coupling on Co–Graphdiyne for Selective CO₂ Reduction

Jofrey J. Masana *

Mwalimu Nyerere University of Agriculture and Technology, P.O Box 976, Musoma,
Tanzania.

**Corresponding authors. E-mail: jofrey.masana@mnuat.ac.tz/masanajay@gmail.com*

1. Supporting Figures

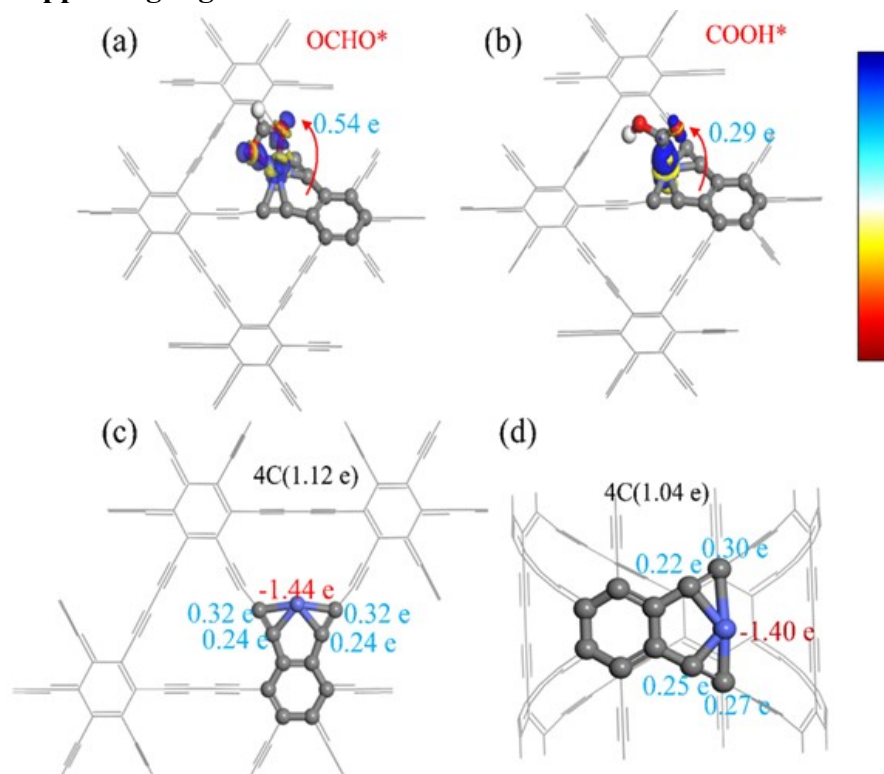


Fig. S1: The charge density difference diagram of T and T1 adsorption intermediate: (a) OCHO*, (b) COOH*, (c) Electronic layout of the active site Co and 4C in the T. (d) Electronic layout of the active site Co and 4C in the T1. Yellow represents charge depletion, and blue represents charge accumulation.

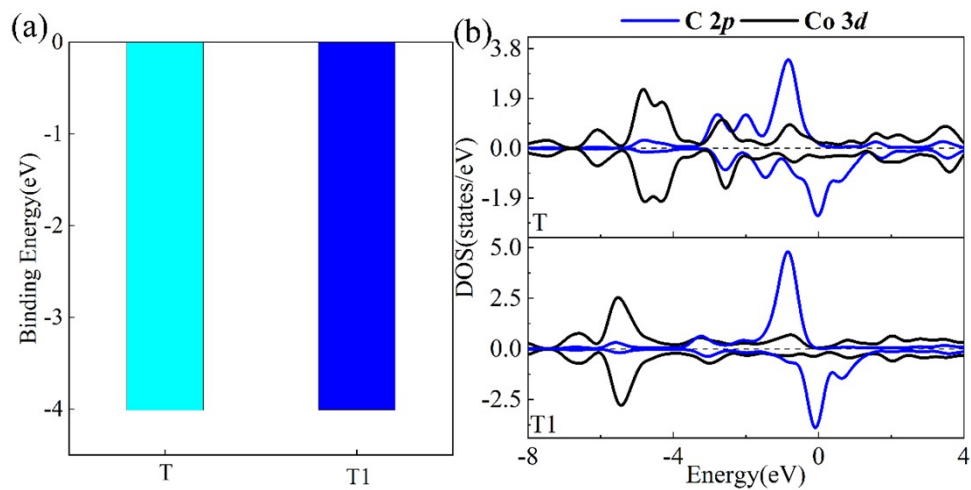


Fig. S2: (a) Comparison of binding energy between Co and substrate in T and T1. (b) The density of states of Co and the surrounding 4C in T and T1.

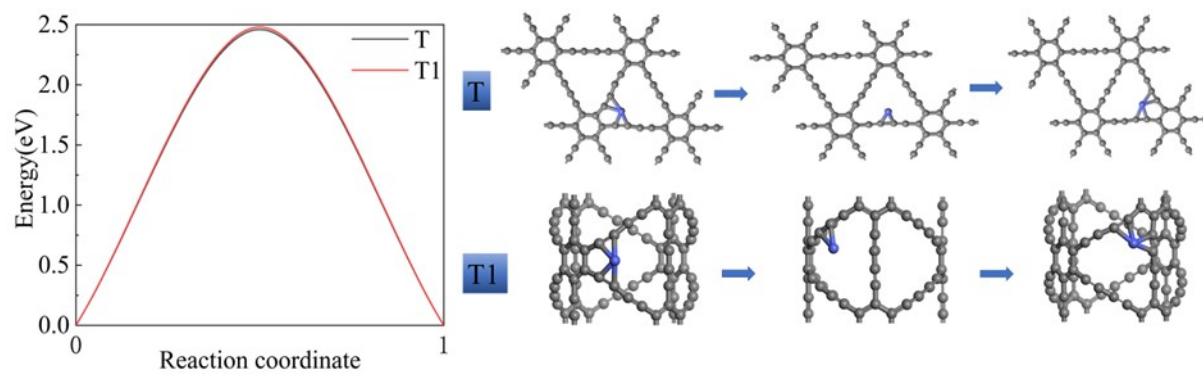


Fig. S3: The migration energy barrier and migration path of metal single atom Co in T and T1.

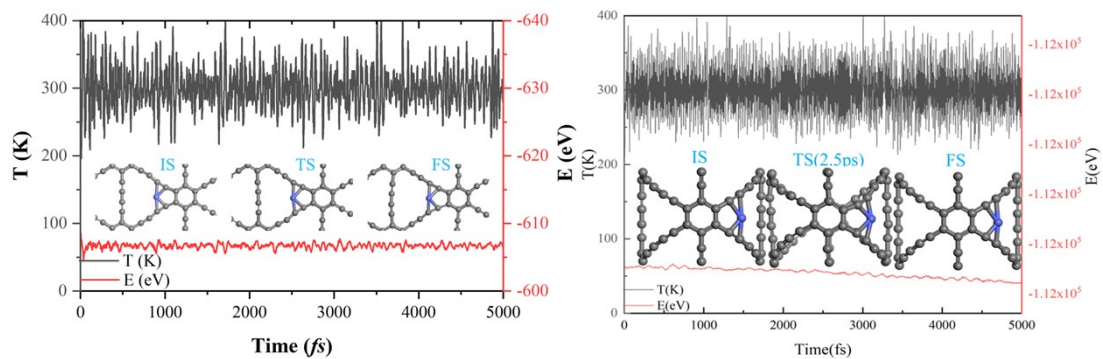


Fig. S4: Molecular dynamics simulation of (a) T and (b) T1 at room temperature, temperature and energy changes with time.

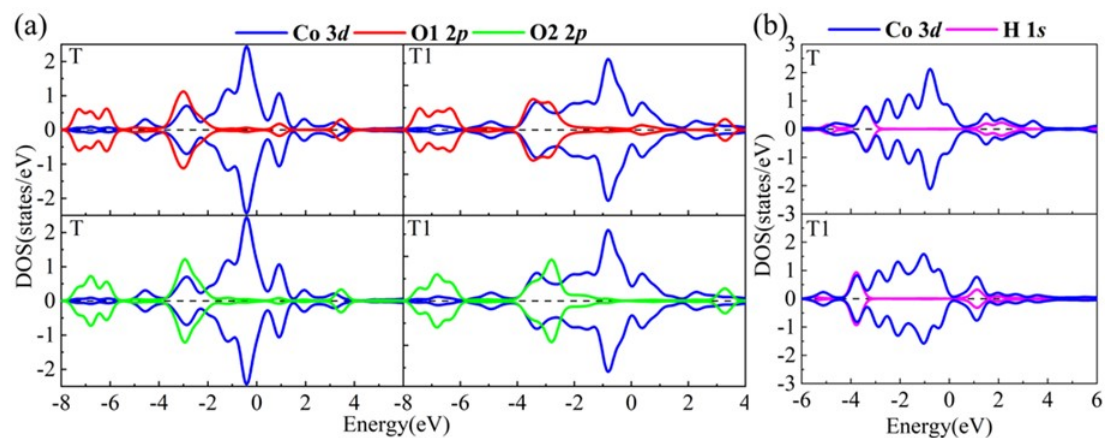


Fig. S5: (a) The density of states of intermediate OCHO* on the surface of T and T1, respectively. (b) The density of states of intermediate H* on the surface of T and T1, respectively.

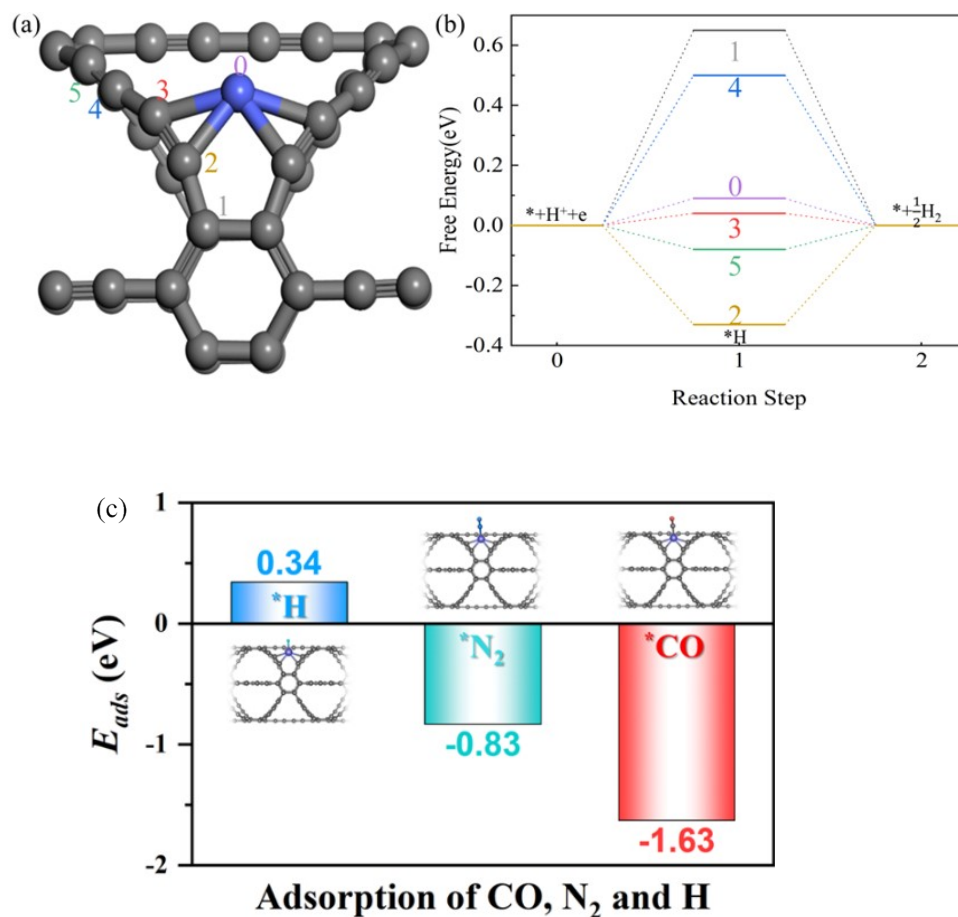


Fig. S6: (a) Possible sites for HER in T1. (b) T1 may be used to compare the performance of HER sites, and (c) adsorption of $*CO$, $*N_2$ and $*H$

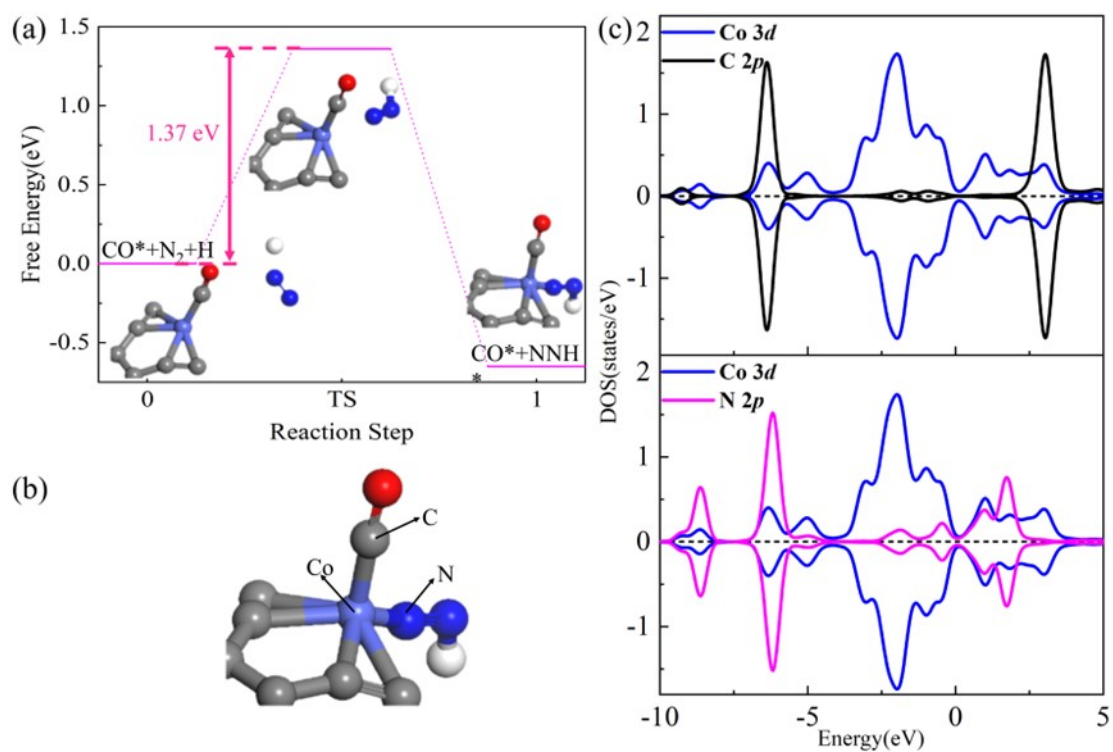
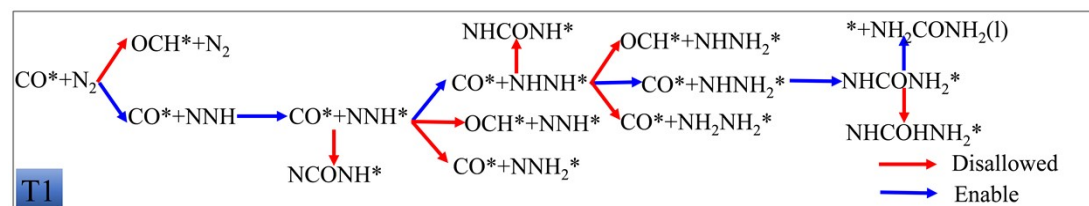
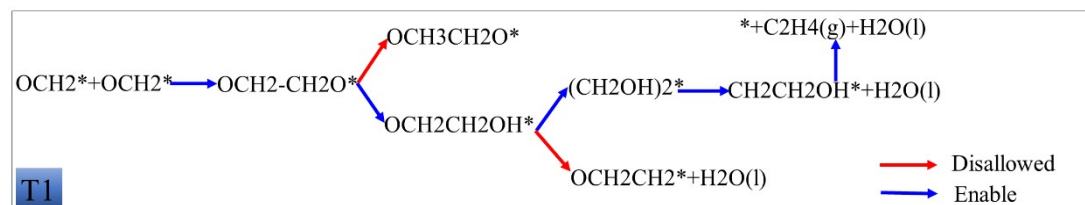
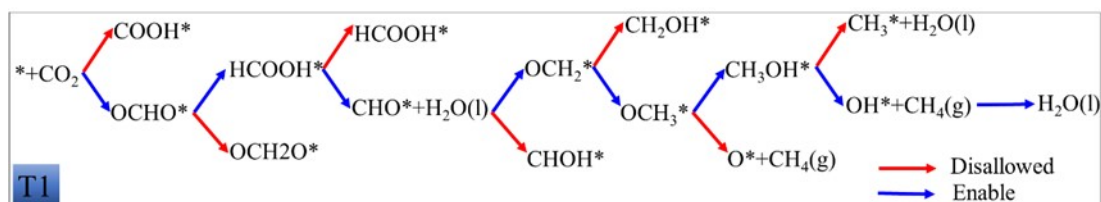
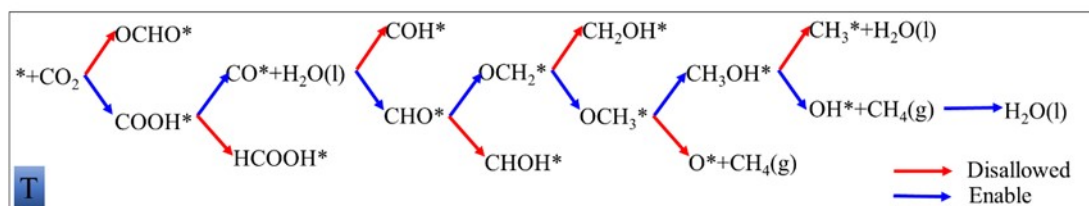


Fig. S7: (a) Transition state energy search of activated N₂. (b) T1 adsorbs the binding site of CO and NNH. (c) The density of states diagram of T1 forming CO* + NNH*.

2. The Schematic Diagram of Path Discrimination in Free Energy Calculation

Calculation

In the whole process of CO₂RR, the major C₁ reduction products include CO, HCOOH, CH₂O, CH₃OH, and CH₄. The formation and release of these products largely depend on the interaction strength between the adsorbed intermediates and the catalyst surface. Here, an adsorption energy higher than approximately -0.5 eV is considered to indicate relatively weak adsorption and therefore facile desorption of the product species. Although this value is not a strict universal criterion, adsorption energies within this range are commonly interpreted in heterogeneous catalysis and electrocatalysis studies as corresponding to weakly bound intermediates with short surface residence times and favorable desorption behavior¹⁻³. In contrast, intermediates with adsorption energies lower than -0.5 eV tend to remain strongly adsorbed and are therefore more likely to undergo further surface reactions. In particular, CH₄ is considered an ideal low-valence C₁ product because once formed, it can readily desorb from the catalyst surface. The desorption tendencies of C₂ and C-N products are also evaluated using the same adsorption-energy criterion.



3. Computational Methods

All calculations were performed using the CASTEP module in Materials Studio based on density functional theory (DFT). The Perdew–Burke–Ernzerhof (PBE) functional within the generalized gradient approximation (GGA) was employed to describe exchange–correlation interactions. Tkatchenko–Scheffler (TS) corrections were applied to account for dispersion interactions between adsorbates and the catalyst surface. The plane-wave ultrasoft pseudopotential method was adopted with a cutoff energy of 400 eV. Convergence thresholds were set to 1.0×10^{-5} eV for total energy, 3.0×10^{-2} eV/Å for stress, and 1.0×10^{-3} eV/Å for atomic displacement. Spin-polarized calculations were performed using a $3 \times 3 \times 1$ k-point mesh for structural optimization and a denser $5 \times 5 \times 1$ mesh for electronic property calculations. A vacuum layer of 14 Å was introduced along the c-axis to eliminate periodic interactions. The valence electron configurations considered were: H ($1s^1$), C ($2s^2 2p^2$), O ($2s^2 2p^4$), and Co ($3d^7 4s^2$).

In order to show the stability of metal Co atoms loaded on graphdiyne, the binding energy (E_b) is more intuitive. The binding energy (E_b) is defined by Formula 1:

$$E_b(\text{Co}) = E_{\text{total}} - E_{\text{Co}} - E_{\text{slab}} \quad (1)$$

where, E_{total} , E_{Co} and E_{slab} are the amount of monoatomic metal Co loaded on the substrate, monoatomic metal Co and graphyne, respectively. The calculated value shows that the negative value indicates that the single atom metal Co tends to combine with the substrate, and the larger the negative value, the easier the combination.

In order to discuss the strength of the interaction between small molecules and the catalyst surface, the adsorption energy (E_{abs}) has a very good description. The adsorption energy (E_{abs}) is defined by Formula 2:

$$E_{\text{abs}}(n) = E_{n\text{-slab}} - E_n - E_{\text{slab}} \quad (2)$$

where, $E_{n\text{-slab}}$, E_n and E_{slab} represent the energy of a small molecule n adsorbed on the catalyst surface, a single small molecule and the catalyst, respectively. The negative

value indicates that the small molecule n tends to adsorb on the surface of the catalyst, and the larger the negative value, the stronger the adsorption capacity.

Because CO₂RR has many reaction paths, in order to simplify the analysis of reaction paths, Gibbs free energy is introduced as a feasible evaluation method. In the process of electron transfer, the reaction energy can be calculated by the standard hydrogen electrode model (SHE) proposed by Norskov and his collaborators.

The relative free energy is calculated according to Formula 3:

$$\Delta G = G[\text{product}] - G[\text{reactant}] - 0.5G[H_2(g)] + eU \quad (3)$$

In the formula, G is Gibbs free energy, U is the voltage applied externally. When the reaction is a process of n protons and electrons transfer, it must be changed. In order to simplify the calculation, it will be compared with the reversible hydrogen electrode, which is $U = 0V$.

The calculation formula of Gibbs free energy of a single system:

$$G = E + ZPE - TS + \int C_p dT \quad (4)$$

where, E is the total energy of the current system, ZPE , TS and $\int C_p dT$ represent the zero-point vibrational energy, entropy and melting at 298.15 K and 1 atm, respectively. Although solvent molecules can stabilize polar intermediates through hydrogen-bonding interactions, particularly in CO₂RR pathways, the present calculations were performed in vacuum due to the large number of CO₂RR reaction pathways considered and to maintain computational consistency. Neglecting solvation effects does not invalidate the calculations, as previous studies have demonstrated that the omission of solvation often preserves the accurate description of electronic structure characteristics and relative energy trends in comparative DFT studies of related catalyst surfaces⁴⁻⁶. Moreover, implicit solvation approaches remain approximate and may not fully capture the complex interfacial hydrogen-bonding environment at electrified interfaces^{7,8}. Nevertheless, it is acknowledged that explicit or implicit solvation could quantitatively influence the adsorption energies of polar intermediates such as *OCHO and *COOH, which should be considered a limitation of the current study.

REFERENCES

1. A. J. Medford, A. Vojvodic, J. S. Hummelshøj, J. Voss, F. Abild-Pedersen, F. Studt, T. Bligaard, A. Nilsson and J. K. Nørskov, *J. Catal.*, 2015, **328**, 36–42.
2. J. K. Nørskov, T. Bligaard, J. Rossmeisl and C. H. Christensen, *Nat. Chem.*, 2009, **1**, 37–46.
3. Y. Jiao, Y. Zheng, M. Jaroniec and S. Z. Qiao, *Chem. Soc. Rev.*, 2015, **44**, 2060–2086.
4. K. Chan and J. K. Nørskov, *J. Phys. Chem. Lett.*, 2015, **6**, 2663–2668.
5. C. D. Taylor, S. A. Wasileski, J.-S. Filhol and M. Neurock, *Phys. Rev. B*, 2006, **73**, 165402.
6. E. Skúlason, G. S. Karlberg, J. Rossmeisl, T. Bligaard, J. Greeley, H. Jónsson and J. K. Nørskov, *Phys. Chem. Chem. Phys.*, 2007, **9**, 3241–3250.
7. M. Zare, M. Saleheen, S. K. Kundu and A. Heyden, *Commun. Chem.*, 2020, **3**, 187.
8. F. Sarabia, C. Gomez Rodellar, B. Roldan Cuenya and A. Heyden, *Nat. Commun.*, 2024, **15**, 8204.